Distribution of volumes and coordination number in jammed matter: mesoscopic ensemble

Ping Wang[1], Chaoming Song[1], Yuliang Jin[1], Kun Wang[1], Hernán A. Makse[1,*]

Levich Institute and Physics Department, City College of New York, New York, NY 10031, US

Abstract

We investigate the distribution of the volume and coordination number associated to each particle in a jammed packing of monodisperse hard sphere using the mesoscopic ensemble developed in Nature **453**, 606 (2008). Theory predicts an exponential distribution of the orientational volumes for random close packings and random loose packings. A comparison with computer generated packings reveals deviations from the theoretical prediction in the volume distribution, which can be better modeled by a compressed exponential function. On the other hand, the average of the volumes is well reproduced by the theory leading to good predictions of the limiting densities of RCP and RLP. We discuss a more exact theory to capture the volume distribution in its entire range. The available data suggests a plausible order/disorder transition defining random close packings. Finally, we consider an extended ensemble to calculate the coordination number distribution which is shown to be of an exponential and inverse exponential form for coordinations larger and smaller than the average, respectively, in reasonable agreement with the simulated data.

1. Introduction

Jammed matter refers to a broad class of physical many-body systems ranging from granular matter to frictionless emulsions, and colloids. These systems share the property that their constitutive particles can be blocked in a configuration far from thermal equilibrium when undergoing a jamming transition. The statistical mechanical description of these materials is based on the volume fluctuations of the system [1] taken to be the conservative quantity instead of energy, as typically done in thermal system. Therefore, the probability distribution of the volume occupied by each jammed particle is of particular interest and many studies have been devoted to investigate them in detail [2, 3, 4, 5, 6, 7, 8].

Recently, a theory of volume fluctuations has been developed at the mesoscopic level providing a relation between the volume occupied by each particle

*Corresponding author
Email address: hmakse@lev.ccny.cuny.edu (Hernán A. Makse)

and its number of contacts [9]. Thus, the distribution of particle volumes in the system is intimately related to the distribution of contacts per particle. In this paper, we calculate the distribution of (orientational) volumes occupied by each particle in a jammed system of monodisperse hard spheres and the distribution of coordination numbers by following the theoretical formalism of [9], which is in turn based on the Edwards statistical mechanics of jamming [1].

The distributions of volumes and contacts in real packings represent ensemble averages in the statistical mechanics sense. Therefore, the distributions depend on the state of the packings specified by their compactivity through a Boltzmann-like probability in the partition function. We show that in two limiting cases of zero and infinite compactivity (corresponding to the random close packing, RCP, and random loose packing, RLP, respectively) the distributions can be obtained in analytical form. Theory predicts that the distribution of orientational volumes is exponential with a mean volume varying with the average coordination number for RLP and constant for RCP. The theoretical predictions are compared with computer generated jammed packings of equal-size spheres for any friction coefficient. We find that the theory well reproduces certain features of the numerical distributions, but not all, in the entire range of volumes.

The mean value of the occupied volumes is well reproduced by the theory. However, we find important deviations between theory and simulations for the higher moments of the distribution. For instance, simulations show a plateau for small volumes while theory predicts an exponential. For intermediate values, the exponential shape seems to provide a good fit to the simulated data and the predicted dependence of the characteristic volume on the coordination number follows partially the theoretical prediction. However, a higher scrutiny shows deviations in the tail of the distribution which is found to decay faster than exponential, having a compressed exponential tail. We conclude that the full understanding of the distribution requires a more precise theory. We discuss how to obtain more exact solutions of the volume distribution which can capture the behavior in the entire ranges of volumes.

On the other hand, the distribution of coordination numbers provides fundamental information of the microscopic packing structures [3, 8, 10, 11, 12], as well as important characteristics of the mesoscopic volume ensemble. In this paper, we study the distribution of coordination numbers by generalizing the ensemble proposed in [9] to include fluctuations in the number of contacts. Theory predicts an exponential decay for large coordination number and an inverse exponential for small coordination number. Computer simulations well reproduce the predictions. Overall, the present paper serves as a critical assessment of the theoretical predictions of the mesoscopic theory towards the development of an exact formulation at the microscopic level that could capture the behavior in the entire range of volume and coordination number fluctuations of jammed matter.

2. Mesoscopic ensemble of jammed matter

In this section, we briefly review the statistical mechanics theory developed at the mesoscopic level in [9], which serves as the theoretical framework for the study of the distributions of volumes and coordination numbers. A theoretical formalism of the volume ensemble is the starting point for the statistical mechanics of jammed matter [13]. The role traditionally played by the energy in thermal systems is replaced by the volume, and a new parameter X, called "compactivity", is introduced as an analogue of temperature. As a consequence, the canonical partition function can be written as:

$$\mathcal{Z}(X) = \int e^{-W/X} g(W) \Theta_W dW, \tag{1}$$

where W is the free volume function, $g(W)$ is the density of jammed states for a given volume W, and Θ_W imposes the jamming condition. It has been shown [9] that the free volume of coarse-grained "quasiparticles" in a monodisperse hard sphere packing has an inverse relation with their coordination number z:

$$W(z) = \frac{2\sqrt{3}}{z} V_g, \tag{2}$$

where V_g is the sphere volume. Since the quasiparticles are coarse-grained over a uniform background field produced by other particles, Eq.(2) should be understood as a mean-field result at the mesoscopic level. Assuming the quasiparticles are independent, we can simplify the partition function Eq.(1) by changing variables:

$$\mathcal{Z}_{\text{iso}}(X) = \int_Z^6 e^{-W(z)/X} g(z) dz. \tag{3}$$

The limit of integration here is given by the isostatic condition [14, 15, 16] over the mechanical coordination number, Z , counting the contacts with nonzero forces. The mechanical coordination number is different from the geometrical coordination number, z, which counts all contacts, even those with zero forces. By definition, it is easy to see that the geometrical coordination number z is always equal or greater than the mechanical coordination number Z, and in general we have $Z \leq z \leq 6$. The mechanical coordination, $Z(\mu)$, depends on the friction, μ, the interparticle friction coefficient, and varies between $Z(0) = 2d = 6$ and $Z(\infty) = d + 1 = 4$ in dimensions $d = 3$. The density of states $g(z)$ is assumed to have an exponential form, $g(z) = (h_z)^{z-2d} = e^{-(z-2d)/z^*}$, with the constant $h_z \ll 1$, representing the typical separation of the configurations in the phase space (analogous to the Planck constant in quantum mechanics). We have $z^* = -1/\ln h_z$. Equation (3) provides a useful tool to calculate the ensemble average of any physical quantity $f(z)$ since

$$f(X, Z) = \frac{1}{\mathcal{Z}_{\text{iso}}} \int_Z^6 f(z) e^{-W(z)/X} g(z) dz. \tag{4}$$

3. PDF of the orientational free volumes

To calculate the volume distribution using the established mesoscopic formalism, we start by introducing the different definitions of the volume associated with each particle necessary to understand the problem. The starting point is the volume of a Voronoi cell associated to each particle. The Voronoi tessellation tiles the entire packing is shown in [17, 9] to be a good candidate for the volume function of jammed matter. The volume function replaces the Hamiltonian in thermal systems, and describes the state of the jammed packings in the ensemble average in the partition function [1, 9]. The Voronoi volume for each particle $\mathcal{W}_i^{\rm vor}$ gives rise to the total volume of the system $\mathcal{W} = \sum_{i=1}^{N} \mathcal{W}_i^{\rm vor}$, when summed up over all the N particles. In terms of the relative coordinates of the particles, $\vec{r}_{ij}$, we have obtained in [17, 9] for monodisperse particles of radius R and volume V_g the following formula for the Voronoi volume:

$$\mathcal{W}_i^{\rm vor} = \frac{1}{3} \oint \left(\min_{\hat{s}\cdot\hat{r}_{ij}>0} (\frac{r_{ij}}{2\hat{s}\cdot\hat{r}_{ij}}) \right)^3 ds. \tag{5}$$

where the integration is performed over the direction $\hat{s}$ forming an angle θ_{ij} with $\vec{r}_{ij}$ as in Fig. 1, and $\cos\theta_{ij} = \hat{s}\cdot\hat{r}_{ij}$. Taking advantage of this integration we can define an orientational Voronoi volume, $\mathcal{W}_i^s$, for a fixed direction $\hat{s}$, satisfying:

$$\mathcal{W}_i^{\rm vor} = \frac{1}{\oint ds} \oint \mathcal{W}_i^s ds = \langle \mathcal{W}_i^s \rangle_s, \tag{6}$$

from which we obtain:

$$\mathcal{W}_i^s \equiv V_g \left(\frac{1}{2R} \min_{\hat{s}\cdot\hat{r}_{ij}>0} \frac{r_{ij}}{\hat{s}\cdot\hat{r}_{ij}} \right)^3. \tag{7}$$

$\mathcal{W}_i^s$ defines the orientational Voronoi volume which is obtained without the integration over $\hat{s}$.

The average of the orientational volume over $\hat{s}$ for a single particle, Eq. (7), is the Voronoi volume, $\langle \mathcal{W}_i^s \rangle_s = \mathcal{W}_i^{\rm vor}$ and the average of the orientational volume over many particles for a fixed $\hat{s}$ is the same as the average of the Voronoi volume over the particles: $\langle \mathcal{W}_i^s \rangle_i = \langle \mathcal{W}_i^{\rm vor} \rangle_i$, in the case of isotropic systems. This last property is useful since it allows the use of the orientational volume to define the ensemble average of the volume fraction without resorting to the use of the Voronoi volume which contains the average over $\hat{s}$ and therefore is more difficult to treat from a theoretical point of view. We therefore promote the use of the orientational volume function $\mathcal{W}_i^s$ as the fundamental quantity to characterize the state of jammed matter instead of $\mathcal{W}_i^{\rm vor}$. It is important to note that the probability densities of $P(\mathcal{W}_i^s)$ and $P(\mathcal{W}_i^{\rm vor})$ in general differ. For instance, as discussed in Fig. 1 the orientational free volume can be for instance zero while the Voronoi free volume cannot. The distribution of Voronoi volume $P(\mathcal{W}_i^{\rm vor})$ can be fitted by a Gamma distribution [18], however, $P(\mathcal{W}_i^s)$ has a different form as shown below.

We define the reduced free orientational volume function as

$$w^s \equiv \frac{\mathcal{W}_i^s - V_g}{V_g}, \tag{8}$$

(we drop the subscript i in w^s for simplicity of notation).

In what follows, we provide a theory for the probability distribution function of the orientational free volume, $P(w^s)$, which is less complex than the full Voronoi volume distribution of Eq. (5). In [17], this distribution is obtained under assumption of uniformity in the packing, making the theory valid at a mesoscopic level of a few particles diameters. This approximation can be seen as defining quasiparticles of free volume w^s capturing the behavior at the mesoscopic distance. Under this approximation the inverse cumulative distribution $P_>$ is obtained (see Eq. (20) in [9] and Eq. (41) in [17]) from where the probability density can be calculated as, $P(w^s) = \frac{d(1-P_>)}{dw^s}$, then

$$P(w^s) = \frac{1}{w} \exp\left(-\frac{w^s}{w}\right), \tag{9}$$

where the average value over the particles,

$$w \equiv \langle w^s \rangle_i = \int w^s P(w^s) dw^s, \tag{10}$$

was found to be directly related to the geometrical coordination number z (Eq. (2)) as :

$$w(z) = \frac{\kappa}{z}, \tag{11}$$

where $\kappa = 2\sqrt{3}$.

We note that

$$\langle w^s \rangle_i = \frac{\langle \mathcal{W}_i^s \rangle_i}{V_g} - 1 = \frac{\langle \mathcal{W}_i^{\text{vor}} \rangle_i}{V_g} - 1. \tag{12}$$

Therefore, the orientational volume w^s captures the behavior of the average volume function and thus can be used as the fundamental variable to define the microstates of the system instead of the more complicated Voronoi volume.

The distribution of Eq. (9) is not the distribution that one would obtain in real packings (generated either experimentally or numerically) corresponding to the ensemble average of Eq. (9). Therefore, further examination is required to derive the distribution of orientational volumes which can be directly compared with real packings; their states determined by the compactivity, X.

Under the volume ensemble point of view [1], the observables in real packings are ensemble average over the Boltzmann distribution function. Using Eq. (4), the probability distribution of volumes in the canonical volume ensemble for a single quasiparticle of orientational volume w is then:

$$P(w^s|X,Z) = \frac{1}{\mathcal{Z}_{\rm iso}} \int_Z^6 P(w^s) \exp\left[-\frac{w(z)}{X}\right] g(z) dz$$
$$= \frac{1}{\mathcal{Z}_{\rm iso}} \int_Z^6 \frac{1}{w(z)} \exp\left[-\frac{w^s}{w(z)}\right] \exp\left[-\frac{w(z)}{X} + \frac{2\sqrt{3}}{w(z)} \ln h_z\right] dz, \quad (13)$$

where we have used the inverse relation Eq. (11) and the exponential density of states $g(z) \sim (h_z)^z$.

This equation cannot be solved analytically for a general (X, Z). However, analytical forms can be obtained in the limiting cases of $X = 0$ (the ground state) and $X \to \infty$: the RCP and RLP lines in the terminology of [9] respectively (see Fig. 2). The advantage of studying these distributions is that they can be checked with simulations or experiments without the use of the compactivity as a fitting parameter.

From Eq. (13), we find along the RCP line, $P_{\rm RCP}(w^s|Z) \equiv P(w^s|X = 0, Z)$:

$$P_{\rm RCP}(w^s|Z) = \sqrt{3} \exp\Big(-w^s\sqrt{3}\Big), \quad Z \in [4, 6], \quad (14)$$

and for the RLP line, $P_{\rm RLP}(w^s|Z) \equiv P(w^s|X \to \infty, Z)$:

$$P_{\rm RLP}(w^s|Z) = \frac{Z}{2\sqrt{3}} \exp\Big(-\frac{w^s Z}{2\sqrt{3}}\Big), \quad Z \in [4, 6]. \quad (15)$$

We note that both limiting distributions coincide at $Z = 6$, the frictionless J-point.

In what follows, we test the above predictions with computer simulations. We generate packings at the jamming transition using the split algorithm explained in [9]. The packings consist of 10,000 spherical equal-size soft particles interacting via Hertz normal forces, Mindlin tangential forces and the Coulomb condition with friction coefficient μ. The mechanical coordination number Z versus the volume fraction ϕ of the generated packings are plotted in Fig. 2 in the framework of the phase diagram of [9]. We change friction from $\mu = 0$ to $\mu \to \infty$ to generate the packings along the RLP line as indicated in the figure with the corresponding change in the mechanical coordination number from $Z(0) = 6$ to $Z(\infty) = 4$. The RCP line is also generated by changing friction but the volume fraction remains constant, as seen in the figure, while the mechanical coordination varies from 6 to 4.

We focus on the calculation of the probability distribution function of w^s for the packings along the RCP-line to test Eq. (14) and along the RLP-line to test Eq. (15). Figure 3 shows the results. Along the RCP-line, shown in Fig. 3a, we find all distributions are the same, independent of friction and Z, as suggested by Eq. (14). On the other hand, the distribution along the RLP line, shown in Fig. 3b, depends on friction and therefore on $Z(\mu)$ as suggested by theory. The exponential dependence seems to be captured upon a first inspection of the data done in a semi-log graph of Figs. 3a and b (arguably better for the RCP

case), at least for intermediate values and the tail of the distribution. In the case of the RLP line (Fig. 3b), the slope of the semi-log plot of the exponential fit has the same dependence on Z as predicted by theory (that is the slope in the semi-log plot increases linearly with Z) but with twice the constant value as predicted by Eq. (15). We find that the exponential fit leads to a tail with characteristic volume $= Z/\sqrt{3}$, twice the value predicted by theory $Z/(2\sqrt{3})$, Eq. (15). However, the linear trend with Z is observed in the data.

On the other hand, the average of the distributions agrees very well with simulations (see below). But when we fix the mean according to theory the exponential tail is inaccurate. Theory either provides the exponential fit with the incorrect average or provides the correct average with the deviations from the exponential fit.

The same situation is observed in Fig. 3a for the RCP line. We force the fitting to be exponential, and then the average value has to be modified from $\sqrt{3} \to 2\sqrt{3}$. The reason for this discrepancy is that the theory does not capture the distribution in the full range of volumes. Figure 3 clearly show a plateau at small values of w^s deviating from the exponential behavior predicted by the theory.

Furthermore, a more strict scrutiny of the data seems to indicate that the exponential fit may not be sufficiently accurate as shown in Figs. 3a and b. While tempting to conclude that the exponential is a good fit to the data (for instance, the fitting in Fig. 3a looks convincing), further scrutiny reveals important deviations in the tail. To visualize the deviations, one should take the plot and look at it, not frontally, but from the side. It is evident that there is a slight curvature in the distributions deviating from the linearity in the semi-log plots. Indeed, the distributions decay slightly faster than the pure exponential decay predicted by theory. The largest evidence of this deviation is perhaps in the tail of the $\mu \to \infty$ data in the RLP, Fig. 3b.

A double log analysis of the data shown in Figs. 4a and 4b reveals that a compressed exponential behaviour might better capture the tail of the distributions above the average value:

$$P(w^s|Z) \sim A \exp\Big[- \Big(\frac{w^s}{w_c}\Big)^{\beta_w} \Big], \quad w^s > w, \tag{16}$$

where $\beta_w \approx 1.5$ is the compressed exponential exponent ($\beta_w = 1$ would be a pure exponential) valid for all the RCP and RLP packings according to Fig. 4a and 4b, w_c is a characteristic volume independent of Z in the RCP packings and depends on Z for the RLP packings, and A is a constant.

We want to stress the difficulties associated with a fit to a compressed (or stretched) exponential function like Eq. (16). A double log plot gives:

$$\ln\Big(- \ln\big(P(w^s|Z)/A\big)\Big) = \beta_w \ln(w^s) - \beta_w \ln(w_c), \tag{17}$$

providing a linear fit with slope β_w. Beyond the inherent subtleties associated to taking a double log of a function in a such a short range, a further complication arises because such a linear fit depends on the value of the constant A. Since

Eq. (16) covers only the tail of the distribution, A cannot be obtained from normalization, remaining as a fitting parameter. The result is a fitting of β_w dependent slightly on A, providing an extra level of difficulty.

Although the compressed exponential seems to fit the data better than the pure exponential, before more theory or numerical/experimental evidence in the limit $N \to \infty$ become available, we are inclined to conclude that the problem is not closed. We note that a similar dichotomy between exponential and compressed/stretched exponential behavior has plagued the study of the distribution of forces in jammed matter since the first studies on the subject [19]. Given the inherent difficulties in any numerical estimation, the dispute will have to eventually be settled when more exact theories become available.

Beyond the distributions of volumes, the theory reproduces very well the average value of the volumes, Eq. (11). Based on the properties of the averages expressed above, there is no need to calculate the full Voronoi volume to obtain the average volume fraction, since the average of the orientational w^s suffices. For instance in the frictionless packing we find $\langle w^s \rangle = 0.561$, which gives a volume fraction $\phi = 1/(1 + \langle w^s \rangle) = 0.641$, in agreement with the direct measurement of the volume fraction of the packing, 0.64.

A full comparison between theory and simulations is given in Fig. 5, where we study the dependence between average volume and coordination number. For each packing along the RLP line we calculate the average orientational volume focusing on the particles with a given z. We also calculate the average over all the particles for a given packing, plotted as the red dots in Fig 5. In practice, we do not measure the geometrical coordination number z but the mechanical coordination number Z. However, we know that for the packings along the RLP line $z \approx Z$ [9] (this is because $h_z \to 0$). Furthermore, the RLP line corresponds to $X \to \infty$ and therefore the prediction of the average volume function, Eq. (11) can be tested directly with these fully random numerical packings, extending this result, valid for a quasiparticle, to the entire packing. Thus, the packings along the RLP line reveal the approximate behaviour of quasiparticles of fixed coordination z. We notice that there could be still some subtleties when comparing Eq. (11), valid for quasiparticles, to the results in packings. Using $\phi^{-1} = w + 1$, we plot the volume fraction in Fig. 5b.

Figures 5a shows that the mean of the distribution of volumes, w, is well captured by the theory of Eq. (11) (see the black dashed line in comparison with the red dots in Fig. 5). This is why the theory provides very good fittings to the values of RCP and RLP in [9]. The agreement can be seen as well in the volume fraction in Fig. 5b, and exists despite the fact that the full distribution presents the deviations discussed above.

Figure 5 presents further interesting results. For a given packing along the RLP-line specified by a fixed friction, there are a variety of particles with varying coordination z, following a well-defined functional relation between the volume occupied by the particle and its coordination number (see for instance the red and blue dashed lines in Fig. 5a corresponding to fittings for the cases $\mu = 0$ and $\mu \to \infty$, respectively). While this plot does not tell us how many particles there are for a given coordination number (see next section) we see that for each

packing, there exists a variety of local volume functions with z ranging from $z = 0$ (since there are some rattlers) up to $z = 11$ (but not 12, interestingly, see below).

The assumptions for the limits of integration in the partition function in [9] or the ensemble average Eq. (3), $Z \leq z \leq 6$, seem to be violated here. However, we have to remember that the theory is mesoscopic and further coarse-graining is needed for these bounds to be more accurate. Regardless, even though the range in z extends further than the bounds, Fig. 5 corresponds to the average for a fixed z but does not tell how many states there are for every z. When these details are properly taken into account, the bounds are approximately satisfied, although fluctuations persist, bringing us to the next Section of this paper.

Focusing around the $z = 12$ point in the figures, we observe that an extrapolation of the fitting to the curve of frictionless packing seems to converge to the green dot in Figs. 5 at $z = 12$ which correspond to the free volume function of FCC, $w_{\mathrm{FCC}} = 0.35135$ (Fig. 5a) and the FCC volume fraction $\phi_{\mathrm{FCC}} = \pi/\sqrt{18} \approx 0.7402$ (Fig. 5b). An extrapolation of the fitting to the infinite friction data seems to pass through the volume fraction of the dodecahedron as indicated by the blue point in Fig. 5, which has also $z = 12$ but slightly larger volume fraction that FCC (the dodecahedron can't tile the space without leaving holes, so the best global packing is still the FCC). We observe that there are no particles in the packings with $z = 12$. Indeed the green and blue points at $z = 12$ in Figs. 5a and b were added by hand and the real curves stop shortly at $z = 11$. The absence of $z = 12$ states indicate the randomized state of the systems.

More importantly, we see that if we extend the theoretical result of Eq. (11) to the ordered region, examining z from $z = 6$ to $z = 12$, the theory does not fit the FCC value. Instead, we obtain $w(z = 12) = 2\sqrt{3}/12 = 0.2886$, below the FCC or dodecahedron value. In principle, this result is expected since the theory assumes random isotropic states while the FCC is an ordered anisotropic packing. However, the absence of a good fitting of the disordered branch through the FCC, together with the fact that the theory fits so well the disordered states, raises the interesting question of the existence of a phase transition between the RCP limit at $z = 6$ and the FCC at $z = 12$. Since packings cannot equilibrate above $z = 6$ without the formation of crystalline regions, we expect an ordered branch from the FCC point towards the RCP point. It seems plausible that there could be a discontinuity from the disordered branch to the ordered branch, the existence of which could determine whether there exist a disorder/order phase transition characterizing the RCP. This scenario has been confirmed by analysis of numerical packings in a recent study [20], which showed that RCP can be interpreted as a "freezing point" in a first-order phase transition between ordered and disordered phases.

To summarize this part of the study, while theory predicts an exponential behavior and approximates well some features of the distribution such as the average value, simulations indicate that a compressed exponential fitting could be also possible. We therefore require more refined theories to account for the full behavior of the volume distribution. The present approach suggests that study

of the ensemble of quasiparticles of fixed coordination number could provide clues to the behavior of the entire system through the Edwards ensemble approach. While new theoretical concepts are required, current attempts indicate that it might be possible to develop a theory of the volume distribution that is exact to, at least, a given coordination shell of particles. It appears that $P(w^s)$ for a fixed z-ensemble might be solved exactly by a brute force approach, since the range of a Voronoi cell is finite. Although, it may contain a large number of variables, the computer should handle such a computation. Such an analysis parallels the Hales proofs of the Kepler's conjecture [21].

4. PDF of the coordination number

Next, we analyze the distribution of coordination number by generalizing the theory of [9] to include fluctuations in z. While we have assumed [9] that every single quasiparticle satisfies the specified bounds: $Z \leq z \leq 6$, below we relax this constraint to extend the bounds to the geometrical coordination of the entire system by considering:

$$N z_{\min} \leq \sum_{i=1}^{N} z_i \leq N z_{\max}, \tag{18}$$

where in the following we set $z_{\min} = Z$ and $z_{\max} = 6$. This new condition implies that it is not possible to consider the single quasiparticle partition function, Eq. (3), and that the full N-particle partition function has to be considered:

$$\begin{aligned} \mathcal{Z} &= \int \dots \int_{N z_{\min} \leq \sum_{i=1}^{N} z_i \leq N z_{\max}} \prod_{i=1}^{N} e^{-w_i(z_i)} g_i(z_i) dz_i \\ &= \int \dots \int_{N z_{\min} \leq \sum_{i=1}^{N} z_i \leq N z_{\max}} \prod_{i=1}^{N} e^{-(z_i/z^* + \beta\kappa/z_i)} dz_i. \end{aligned} \tag{19}$$

We have $z^* = -1/\ln h_z$, the inverse compactivity $\beta = 1/X$ and the coupling constant

$$B = \frac{\beta\kappa}{z^*}. \tag{20}$$

Then, the ensemble average of the probability distribution function of the geometrical coordination number, $P(z)$, is

$$\begin{aligned} P(z) &\equiv \left\langle \frac{1}{N} \sum_{i=1}^{N} \delta(z - z_i) \right\rangle \\ &= \frac{1}{\mathcal{Z}} \int \dots \int_{(N z_{\min} - z) \leq \sum_{i=1}^{N-1} z_i \leq (N z_{\max} - z)} \prod_{i=1}^{N-1} e^{-(z_i/z^* + \beta\kappa/z_i)} dz_i, \end{aligned} \tag{21}$$

We obtain:

$$P(z) = \frac{\mathrm{Erf}(\frac{\sqrt{N-1}(z'_{\max}-\mu)}{\sqrt{2}\sigma}) + \mathrm{Erf}(\frac{\sqrt{N-1}(\mu-z'_{\min})}{\sqrt{2}\sigma})}{\mathrm{Erf}(\frac{\sqrt{N}(z_{\max}-\mu)}{\sqrt{2}\sigma}) + \mathrm{Erf}(\frac{\sqrt{N}(\mu-z_{\min})}{\sqrt{2}\sigma})} e^{-(z/z^* + \beta\kappa/z)}, \tag{22}$$

with the following constants:

$$\begin{aligned} z'_{\max} &\equiv (Nz_{\max} - z)/(N-1) \approx z_{\max} + (z_{\max} - z)/N, \\ z'_{\min} &\equiv (Nz_{\min} - z)/(N-1) \approx z_{\min} + (z_{\min} - z)/N, \end{aligned} \tag{23}$$

and $\mathrm{Erf}(x)$ the Gauss error function.

The constants μ and σ in Eq. (22) are significant because they represent the mean and standard deviation of the a Gaussian expansion in a saddle-point approximation of the inverse Fourier transform of the partition function allowing the calculation of the free-volume density. They are:

$$\mu = z^* B^{1/2} \frac{K_1(2B^{1/2})}{K_0(2B^{1/2})}, \tag{24}$$

which is the same as the ensemble average of the coordination number, and

$$\sigma^2 \equiv {z^*}^2 B \left(\frac{K_2(2B^{1/2})}{K_0(2B^{1/2})} - \frac{K_1(2B^{1/2})^2}{K_0(2B^{1/2})^2} \right), \tag{25}$$

where $K_n(a)$ is the modified Bessel function of the second kind:

$$\int_0^\infty x^n e^{-\frac{a}{2}(x+1/x)} dx = 2K_n(a). \tag{26}$$

Next, we consider the approximations of Eq. (22) for two cases: When $z_{\max} - \mu < \mu - z_{\min}$, then $\mu > (z_{\max} + z_{\min})/2$, and we obtain:

$$P(z) \sim \exp\left[-\frac{1}{z^*} \left(z\,(2 - \bar{w}/w_{\min}) + \frac{1}{z}\frac{\kappa^2}{\bar{w}^2} \right) \right], \tag{27}$$

or otherwise, we obtain:

$$P(z) \sim \exp\left[-\frac{1}{z^*} \left(z\,(2 - \bar{w}/w_{\max}) + \frac{1}{z}\frac{\kappa^2}{\bar{w}^2} \right) \right], \tag{28}$$

where $\bar{w}$ is the ensemble average of the volume function (which depends on β, or compactivity X), $w_{\min} = \kappa/z_{\max}$ and $w_{\max} = \kappa/z_{\min}$.

In the following we consider the distribution functions at two special points on the phase diagram and compare them to the numerical simulations. At the frictionless J-point and the infinitely frictional L-point (see Fig. 2), the distributions reduce to simple forms. For the RCP J-point, $X = 0$ and the system has the minimum average volume and maximum average coordination number, therefore, $\bar{w} \sim w_{\min}$ and $u \sim z_{\max}$. From Eq. (27) We find:

$$P_{\mathrm{RCP}}(z) \sim \exp\left[-\frac{1}{z^*} \left(z + \frac{z_{\max}^2}{z} \right) \right]. \tag{29}$$

For the RLP L-point, $X \to \infty$ and the system has the maximum average volume and minimum average coordination number, therefore, $\bar{w} \sim w_{\max}$ and $u \sim z_{\min}$. From Eq. (28), we find:

$$P_{\mathrm{RLP}}(z) \sim \exp\left[-\frac{1}{z^*}\left(z + \frac{z_{\min}^2}{z}\right)\right]. \tag{30}$$

We test these forms with the computer generated packings at the J-point and L-point. The constant z^* is treated as a fitting parameter since it determines the density of states and is difficult to know a priori. Figure 6 shows the result. The lin-lin plot of Fig. 6a shows that the distribution near the average value is well approximated by the theory for both points. To investigate the tails of the distributions, Fig. 6b plots a semi-log curve. While some deviations are observed, the fit is still reasonable except for the larger coordination number of J-point and smaller coordination number of L-point, which are very rare, about 10^{-2} less probable than the most probable value.

5. Conclusions

We have presented the predictions of the mesoscopic theory presented in [9] concerning the probability distribution of the orientational volumes in jammed matter. The theory captures very well the average volume and indeed gives rise to good predictions of the RCP and RLP volume fraction as shown in [9]. However, when comparing the full distribution we find important deviations. For instance, computer simulations are able to detect slight deviations from the pure exponential behaviour predicted by theory. This deviation could be better approximated by a compressed exponential behavior, although a more conclusive fitting necessitates a more precise theory or simulations in the large scale limit. The plateau observed in the volume distribution is not captured by the theory either. There is evidence that this plateau might originate from the spatial correlations between the first and second layer particles, which indicates that further progress could come from a systematic analysis of higher level coarse-graining. For example, by explicitly treating the second-layer neighbors, it is possible to improve the distribution functions predicted by the theory. This approach is particularly appropriate for two-dimensional systems, since the free variables are significantly reduced in the 2d case.

On the other hand, the behavior of the probability distribution of coordination number is captured well by the theory. Here, the mesoscopic theory of [9], considering restricted bounds for each quasiparticle, is extended to allow for coordination number fluctuations, by imposing the bounds to the entire system. Such a problem can be solved under several approximations and predicts a mixed exponential forms that are well reproduced by the simulations at the J and the L-point.

Why does the theory capture the contact distribution better than the volume distribution? The distribution of contacts is an ensemble average based on the states characterized by $w(z)$. Since this function is quite accurate, the contact

distribution follows. On the other hand, the volume distribution is based on the uniform approximations done on [17], and therefore is not quite exact. The full distribution of volumes is where more theoretical developments are required.

Acknowledgements

This work is supported by NSF-CMMT, and DOE Geosciences Division. We thank C. Briscoe and L. K. Gallos for a critical reading of this manuscript.

References

References

[1] Edwards S F 1994 The role of entropy in the specification of a powder *Granular matter: an interdisciplinary approach* ed A Mehta (New York: Springer-Verlag) pp 121-140

[2] Finney J L 1970 *Proc. R. Soc. Lond. A* **319** 479

[3] Aste T, Saadatfar M and Senden T J 2006 *J. Stat. Mech.* P07010

[4] Lechenault F, da Cruz F, Dauchot O and Bertin E 2006 *J. Stat. Mech.* P07009

[5] Makse H A, Brujić J and Edwards S F 2004 Statistical Mechanics of Jammed Matter *The Physics of Granular Media* ed H Hinrichsen and D E Wolf (Wiley-VCH)

[6] Frenkel G, Blumenfeld R, Grof Z and King P R 2008 *Phys. Rev. E* **77** 041304

[7] Schröter M, Goldman D I and Swinney H L 2005 *Phys. Rev. E* **71** 030301

[8] Brujić J, Song C, Wang P, Briscoe C, Marty G and Makse H A 2007 *Phys. Rev. Lett.* **98** 248001

[9] Song C, Wang P and Makse H A 2008 *Nature* **453** 606

[10] Clusel M, Corwin E I, Siemens A O N and Brujić J 2009 *Nature* **460** 611

[11] Zhang H P and Makse H A 2005 *Phys. Rev. E* **72** 011301

[12] Troadec H, Radjai F, Roux S and Charmet J C 2002 *Phys. Rev. E* **66** 041305

[13] Edwards S F and Oakeshott R B S 1989 *Physica A* **157** 1080

[14] Alexander S 1998 *Phys. Rep.* **296** 65

[15] Moukarzel C F 1998 *Phys. Rev. Lett.* **81** 1634

[16] Edwards S F and Grinev D V 1999 *Phys. Rev. Lett.* **82** 5397

[17] Song C, Wang P, Jin Y and Makse H A 2010 *Physica A* **389** 4497

[18] Aste T, Di Matteo T, Saadatfar T M, Senden T J, Schröter M and Swinney H L 2007 *Europhys. Lett.* **79** 24003

[19] Tighe B P, Snoeijer J H, Vlugt T J H and van Hecke M 2010 *Soft Matter* **6** 2908-2917

[20] Jin Y and Makse H A 2010 *Physica A* **389** 5362

[21] Hales T C http://arxiv.org/-abs/math.MG/9811078

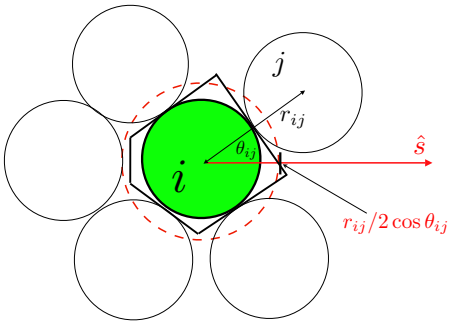

Figure 1: Schematics of the Voronoi volume and the orientational volume associated with particle i. The boundary of the Voronoi cell (shown in 2d for simplicity) corresponds to the irregular pentagon in black which defines $\mathcal{W}_i^{\rm vor}$. The limit of the Voronoi cell of particle i in the direction $\hat{s}$ is the minimum of $r_{ij}/2\cos\theta_{ij}$ over all the particles in the packing, as indicated. This defines the orientational volume $\mathcal{W}_i^s$ which is the volume of the sphere of radius $r_{ij}/2\cos\theta_{ij}$ defined by the dash red circle in the figure. The Voronoi volume is the integration of the orientational volume over $\hat{s}$ as in Eq. (6). Notice that w^s, the orientational free volume associated with $\mathcal{W}_i^s$ defined in Eq. (8), ranges from zero (when the orientational volume coincides with the volume of the central ball, that is when the direction $\hat{s}$ coincides with a contact point) to in principle ∞ for an isolated ball, although the maximum w^s in a jammed system is, of course, bounded by the free space given by the first or second coordination shell. The Voronoi free volume, on the other hand, cannot be zero, by definition.

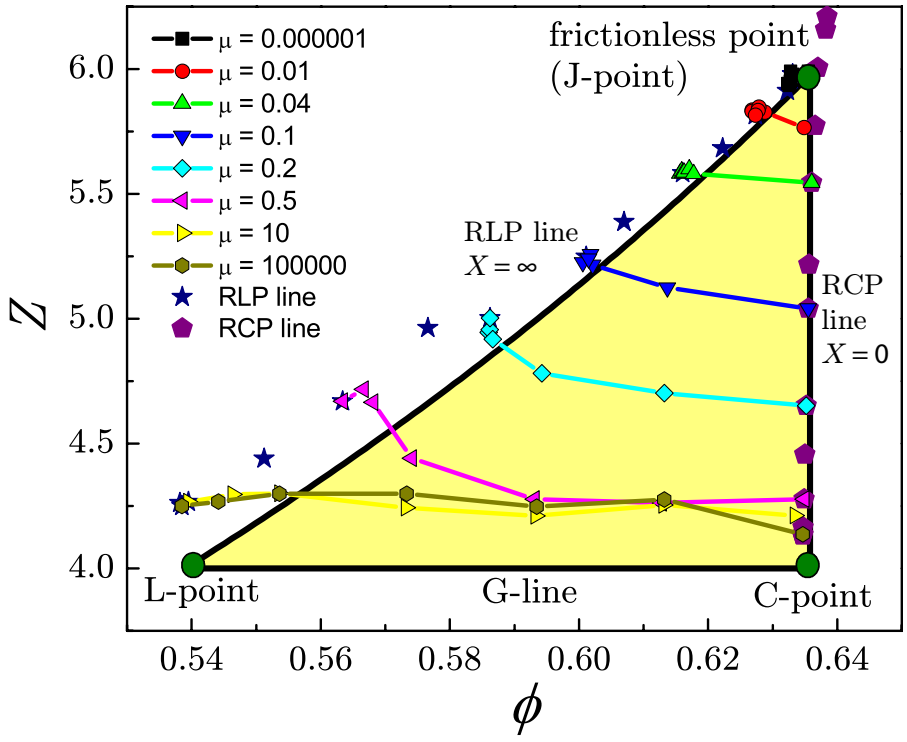

Figure 2: Computer generated packings arranged in the phase diagram of [9]. The packings are used to calculate the distribution of orientational volumes and coordination number. We concentrate our study on packings generated with different friction as indicated in the figure following the RLP line from the J point to the L point and the RCP line from the J point to the C point.

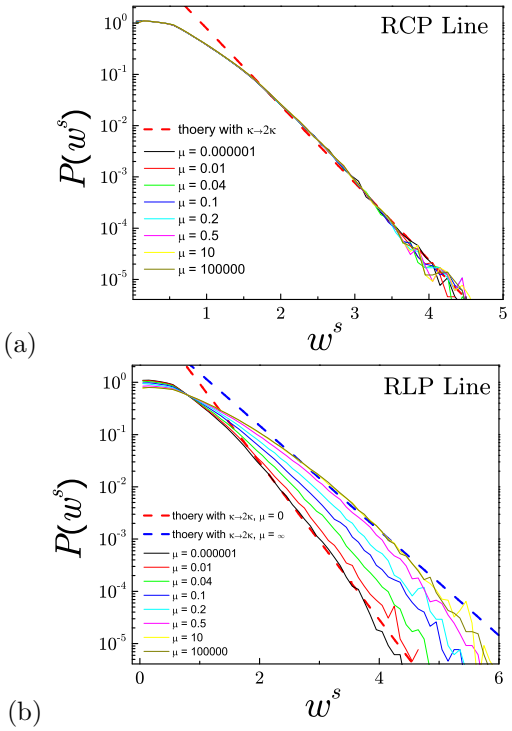

Figure 3: PDF of w^s. Exponential fit in a semilog plot. (a) We plot the results for the distribution of the packings along the RCP line with different values of friction, as indicated in the figure (see Fig 2). The red dashed line is a fit with the theoretical prediction $P_{\rm RCP}(w^s)$, Eq. (14), but with the inverse characteristic volume or slope of $2\sqrt{3}$ instead of $\sqrt{3}$ as predicted by the theory. (b) Same as (a) but for the packings along the RLP line in Fig. 2 prepared with different μ. The red and blue dashed lines are fits to the theoretical prediction $P_{\rm RLP}(w^s)$, Eq. (15), but with the inverse characteristic volume or slope replaced from $Z/(2\sqrt{3}) \to Z/\sqrt{3}$, twice as predicted by the theory like in (a). The red line is for $\mu = 0$ and has slope $2\sqrt{3}$. The blue line is for $\mu \to \infty$ and has slope $4/\sqrt{3}$.

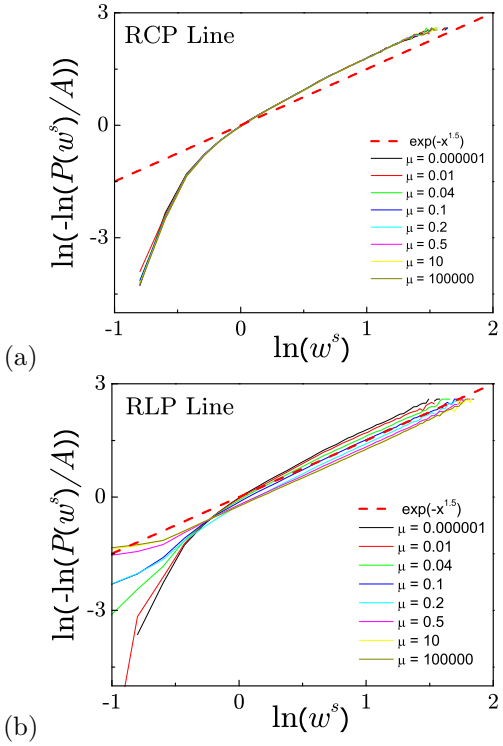

Figure 4: PDF of w^s. Compressed exponential fit in a double log plot. The results are the same as in Fig. 3 but now reploted in a double log plot to obtain the compressed exponential fitting exponent β which is extracted from the sloe of such a plot, as explained in the text. (a) PDF for the packings along RLP-line. (b) PDF for the packings along the RLP-line.

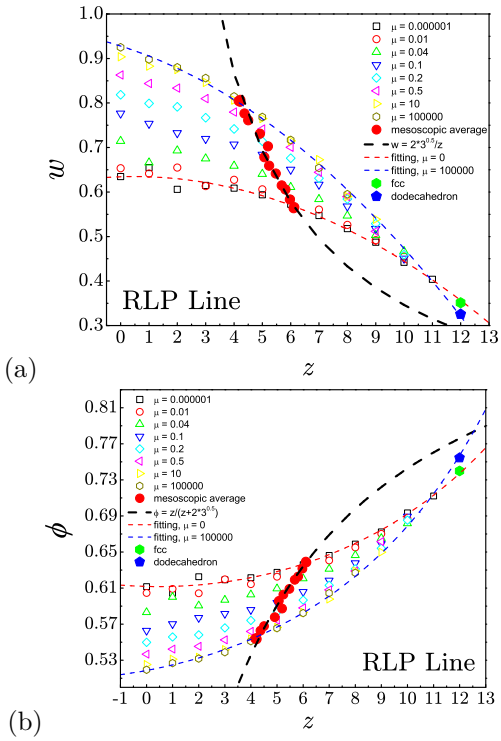

Figure 5: Relation between local volume per particle and its coordination number for (a) the volume function and (b) the volume fraction. We use the packings along the RLP line with the friction as indicated and we calculate the volume function binning the data by the coordination number of the particles. The red dots correspond to the average over all the particles in the packing of the volume function which fits the theory very well. The red and blue dashed lines are logarithmic-like fittings to the data and we add the value at $z = 12$ for the FCC and the dodecahedron. The data from the packings goes only up to $z = 11$, indicating the absence of ordered structures.

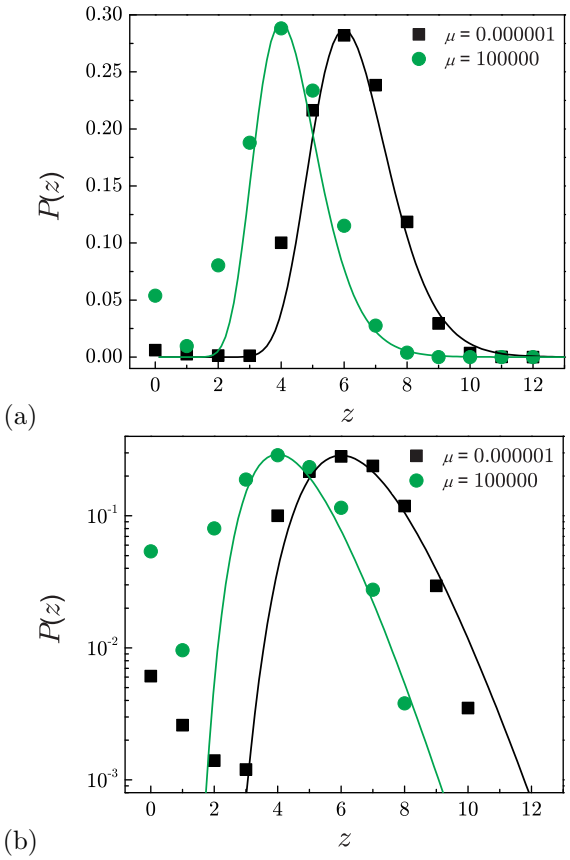

Figure 6: $P(z)$: comparison between theory and simulations in (a) a lin lin plot and (b) a semi-log plot to appreciate better the tail of the distribution. We plot the systems at the J-point ($\mu = 0$) and L-point ($\mu = \infty$) in Fig. 2. we use a fitting parameter $z^* = 0.5$ in Eqs. (29) and (30).